



PERGAMON

www.elsevier.com/locate/watres

Wat. Res. Vol. 34, No. 12, pp. 3197–3203, 2000
© 2000 Elsevier Science Ltd. All rights reserved
Printed in Great Britain
0043-1354/00/\$ - see front matter

PII: S0043-1354(00)00077-4

HYPOIODOUS ACID: KINETICS OF THE BUFFER-CATALYZED DISPROPORTIONATION

YVES BICHSEL and URS VON GUNTEN*

Swiss Federal Institute for Environmental Science and Technology EAWAG, CH-8600, Dübendorf, Switzerland

(First received 1 June 1999; accepted in revised form 1 September 1999)

Abstract—The reactivity of hypiodous acid (HOI) is an important factor for the fate of iodine in oxidative drinking water treatment. The possible reactions of HOI are its disproportionation, its oxidation to iodate (IO_3^-), or the reaction with natural organic matter (NOM). The latter reaction may result in the formation of iodoorganic compounds which are frequently responsible for taste and odor problems. The acid dissociation constant (pK_a) of HOI has been determined spectrophotometrically as 10.4 ± 0.1 ($T = 25^\circ\text{C}$; $I = 50 \text{ mM}$). Kinetic constants and a new rate law for the disproportionation of HOI as catalyzed by hydrogencarbonate, carbonate, and borate are presented. In the pH range 7.6–11.1, the main uncatalyzed reactions are $\text{HOI} + \text{HOI}$ ($k_1 = 0.3 \text{ M}^{-1} \text{ s}^{-1}$) and $\text{HOI} + \text{OI}^-$ ($k_2 = 15 \text{ M}^{-1} \text{ s}^{-1}$). The buffer-catalyzed reaction step was found to be second-order in HOI and first-order in the buffer anion. The following rate constants were deduced: $\text{HOI} + \text{HOI} + \text{HCO}_3^-$: $50 \text{ M}^{-2} \text{ s}^{-1}$; $\text{HOI} + \text{HOI} + \text{CO}_3^{2-}$: $5000 \text{ M}^{-2} \text{ s}^{-1}$; $\text{HOI} + \text{HOI} + \text{B}(\text{OH})_4^-$: $1700 \text{ M}^{-2} \text{ s}^{-1}$. All these rate constants result in half-lives for HOI of 10–1000 days under typical drinking water conditions. © 2000 Elsevier Science Ltd. All rights reserved

Key words—acid dissociation constant, disproportionation, drinking water, iodoorganic compounds, iodine, taste and odor

INTRODUCTION

In the late 1980s, it was observed that taste and odor problems in drinking waters were frequently linked to the presence of iodoorganic compounds (Hansson *et al.*, 1987; Bruchet *et al.*, 1989). The identified compounds were iodo-trihalomethanes (I-THMs) which can be formed in a reaction of hypiodous acid (HOI) with natural organic matter (NOM). It has been estimated that I-THMs contribute up to 25% of the cases of bad taste and odor in drinking waters in France (Suez Lyonnaise des Eaux, 1993). The most problematic I-THM is iodoform (CHI_3) with an organoleptic threshold concentration of $1 \mu\text{g l}^{-1}$ (Bruchet *et al.*, 1989). This concentration has to be compared to the total iodine concentration in water resources which is usually in the range of $0.5\text{--}10 \mu\text{g l}^{-1}$, but which can exceed $50 \mu\text{g l}^{-1}$ in certain ground waters near the sea coast or under special geological circumstances (Fuge and Johnson, 1986). The most abundant iodine species in natural waters are iodide (I^-) and iodate (IO_3^-) (Fuge and Johnson, 1986).

In oxidative drinking water treatment, I^- is first

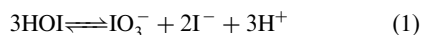
oxidized to HOI in the presence of ozone (Garland *et al.*, 1980), chlorine (Nagy *et al.*, 1988), and chloramine (Kumar *et al.*, 1986) in a fast reaction. In a second step, some of these disinfectants oxidize HOI to IO_3^- . Ozone oxidizes I^- to IO_3^- within 1 s under typical drinking water treatment conditions (Bichsel and von Gunten, 1999a). In chlorination processes, the oxidation of HOI to IO_3^- is slower and occurs within minutes to hours. Chloramine does not oxidize HOI at all (Bichsel and von Gunten, 1999a). Chlorine dioxide oxidizes I^- to I radicals which involves a different chemistry than the other disinfectants (Fabian and Gordon, 1997). The fate of I radicals in drinking water is unknown.

HOI can also disproportionate to IO_3^- and I^- or, as mentioned above, react with NOM that may lead to iodoorganic compounds. All these reactions of HOI—its oxidation to IO_3^- , its disproportionation to IO_3^- and I^- , and the reaction with NOM—are in kinetic competition. The relative reaction rates of these reactions determine the fraction of iodine found as IO_3^- and I_{org} . Whereas the oxidation of HOI has been described previously (Bichsel and von Gunten, 1999a) and reaction kinetics of HOI with organic compounds are still under investigation, the present study will focus on the disproportionation.

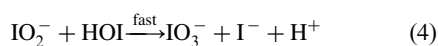
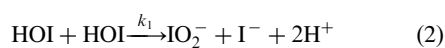
The disproportionation of HOI can be described

*Author to whom all correspondence should be addressed.
Tel.: +41-1-823-5270; fax: +41-1-823-5028; e-mail: vongunten@eawag.ch

by the equilibrium:



The equilibrium constant of this reaction is 6×10^{-11} (Myers and Kennedy, 1950). At $\text{pH} > 5$, HOI is, therefore, thermodynamically unstable since the equilibrium is forced to the right side of equation (1). However, the formation of the reaction products IO_3^- and I^- is kinetically controlled. The kinetics of this reaction have been observed to be second-order in $[\text{HOI}]_{\text{tot}}$, the sum of $[\text{HOI}]$ and $[\text{OI}^-]$ (Thomas *et al.*, 1980; Wren *et al.*, 1986; Truesdale, 1997; Urbansky *et al.*, 1997). The reaction mechanism is generally described by a series of reactions [equations (2–4)] with the rate-limiting step being equations (2) or (3).



The overall reaction (1) is catalyzed by buffers such as phosphate, borate, or acetate (Buxton and Sellers, 1985; Truesdale and Canosa-Mas, 1995; Urbansky *et al.*, 1997). Because different interpretations for the catalysis are given in the literature, it has been difficult to find consistent rate constants for the catalyzed and uncatalyzed reaction steps. Therefore, the reported rate constants k_1 at buffer concentrations of 0–150 mM vary within a wide range of $< 2 \text{ M}^{-1} \text{ s}^{-1}$ to $1000 \text{ M}^{-1} \text{ s}^{-1}$ (Thomas *et al.*, 1980; Truesdale, 1997; Urbansky *et al.*, 1997). The rate constants k_2 were found to be between $40 \text{ M}^{-1} \text{ s}^{-1}$ and $10^6 \text{ M}^{-1} \text{ s}^{-1}$ (Wren *et al.*, 1986; Truesdale and Canosa-Mas, 1995). A value of $2200 \text{ M}^{-2} \text{ s}^{-1}$ was found for the catalysis of the reaction $\text{HOI} + \text{HOI}$ by borate buffer (Buxton and Sellers, 1985).

Because the disproportionation can either occur through the reaction $\text{HOI} + \text{HOI}$ [equation (2)] or $\text{HOI} + \text{OI}^-$ [equation (3)], the dissociation constant of HOI is of particular importance. The pK_a of HOI has previously been indirectly determined as 10.6 ± 0.8 (Chia, 1958).

To assess the fate of HOI in natural waters, we investigated the kinetics of the disproportionation of HOI as catalyzed by borate, hydrogencarbonate, and carbonate. Since the disproportionation strongly depends on the acid-base speciation of HOI, we also redetermined the pK_a of HOI.

EXPERIMENTAL

All experiments were performed in double-distilled water. pH measurements were carried out with a Ross

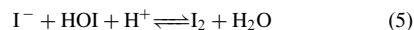
electrode (ATI Orion, Boston, MA) and a Metrohm 632 pH-meter (Metrohm, Herisau, Switzerland) which was calibrated with standard buffer solutions (Merck; $\text{pH} = 6.98, 8.95, 9.94, 11.88$). Spectrophotometric measurements were performed on a Uvikon 940 spectrophotometer (Kontron Instruments, Eching, Germany). HOI is not a stable compound (disproportionation). It was freshly produced directly in the reaction vessel through hydrolysis of I_2 or through oxidation of I^- by HOCl.

Dissociation constant of HOI

The pK_a of HOI was determined spectrophotometrically by measuring the pH-dependence of the UV-absorbance at 220–250 nm ($\text{pH} = 8.7\text{--}11.5$, $25 \pm 2^\circ\text{C}$) in a flow-through cell. It was not possible to perform the measurements in a static cell because of the depletion of HOI/OI^- , due to fast disproportionation under the applied conditions. Buffered solutions of OCl^- (0.2–1 mM) and I^- solutions (0.023–0.46 mM) were delivered with two Dosimats (Metrohm, Herisau, Switzerland) and mixed in a mixing tee prior to the photometric cell. HOI was formed by oxidation of I^- with OCl^- ($k = 4.4 \times 10^{15} \text{ M}^{-1} \text{ s}^{-1} \times [\text{H}^+]$; Kumar *et al.*, 1986) within 80 μs –250 ms (half-life of I^-). The residence times in the cell were 8 s (pathlength 50 mm) and 1.2 s (pathlength 5 mm). The concentration of the NaOCl stock solution (Aldrich) was determined as 5.6% with direct photometry of HOCl at 233 nm ($\epsilon = 100 \text{ M}^{-1} \text{ cm}^{-1}$) (Soulard *et al.*, 1981). The buffer (phosphate) concentration varied from 14 to 17 mM to yield a constant ionic strength of 50 mM. $[\text{OCl}^-]$ was in excess relative to $[\text{I}^-]$ (molar ratio $[\text{OCl}^-]:[\text{I}^-] = 1.1\text{--}9$) to ensure the instantaneous oxidation of I^- to HOI without transient I_2 formation. However, the excess of OCl^- did not lead to significant IO_3^- formation within the residence time of the solution in the flow-through cell (Bichsel and von Gunten, 1999a). The resulting pH was measured at the outlet of the flow-through cell.

Disproportionation kinetics of HOI

The disproportionation of HOI was investigated at $[\text{HOI}]_{\text{tot}} = [\text{HOI}] + [\text{OI}^-] = 0.8\text{--}76 \mu\text{M}$ and at $\text{pH} = 7.6\text{--}11.1$ in 100 ml batch reactors at $25 \pm 2^\circ\text{C}$. The desired $[\text{HOI}]_{\text{tot}(t=0)}$ was achieved by adding an aqueous I_2 solution ($\approx 1 \text{ mM}$, standardized by photometry: $\epsilon = 746 \text{ M}^{-1} \text{ cm}^{-1}$ at 460 nm; Awtrey and Connick, 1951) to a buffered solution (2–30 mM of borate or carbonate/hydrogencarbonate). Under these conditions, I_2 hydrolyzes immediately to HOI/OI^- and I^- [reaction (5)]. Because of the lower $[\text{HOI}]$, the disproportionation was, however, slower than for the conditions that we applied to determine the pK_a . During the reaction time of the disproportionation (10–50 h), aliquots of the solutions were withdrawn and measured photometrically in excess of KI (0.15 M), where HOI and OI^- are quantitatively transformed to I_3^- .



The equilibrium constants for reactions 5 and 6 are $K_5 = 1.84 \times 10^{12}$ and $K_6 = 724$, respectively (Burger and Liebafsky, 1973). I_3^- was detected at 351 nm in a 4 cm cell with a molar absorption coefficient of $25,700 \text{ M}^{-1} \text{ cm}^{-1}$ (Bichsel and von Gunten, 1999b), which allowed us to measure $[\text{HOI}]_{\text{tot}} \geq 1 \mu\text{M}$.

To prevent the presence of CO_2 in the reaction solution, we purged the solutions with N_2 prior to the beginning of the experiment and flushed the head-space of the reaction vessels when taking samples during the reaction time. Uptake of CO_2 leads to carbonate and hydrogencarbonate in the reaction solution, which has a catalytic effect on the disproportionation.

In one experiment, the formation of IO₃⁻ was determined by quenching the disproportionation by H₂O₂ (H₂O₂ + HOI → I⁻ + H⁺ + H₂O + O₂). IO₃⁻ was measured by ion chromatography and postcolumn reaction with a UV/Vis-detection (Bichsel and von Gunten, 1999b). For the anion separation step, an AG-S9 column (Dionex) was used. The postcolumn reaction yields I₃⁻ by reduction of IO₃⁻ to HOI, followed by reactions (5) and (6). I₃⁻ can be measured by UV/Vis-detection at 288 or 351 nm. The detection limit for IO₃⁻ in natural waters was 0.1 μg l⁻¹ (0.6 nM) (Bichsel and von Gunten, 1999b).

RESULTS AND DISCUSSION

Dissociation constant of HOI

Figure 1 shows five of the recorded spectra of HOI/OI⁻ between pH 9.3 and 11.5 which have been corrected for the background absorbance of phosphate and OCl⁻. The molar absorption coefficients of HOI and OI⁻ in the range of 250 to 220 nm increase from 150 to 1650 M⁻¹ cm⁻¹ for HOI and from 300 to 5100 M⁻¹ cm⁻¹ for OI⁻. In our experiments, the wavelength region for best measurements was limited due to interferences by absorbance of HOCl and OCl⁻ since it was added in excess of I⁻ for the production of HOI. Both HOCl and OCl⁻ absorb significantly at wavelengths > 250 nm. The lower wavelength region was limited by the absorbance of the buffer (phosphate) at λ < 220 nm. An accurate data evaluation was only possible at wavelengths with no interferences and maximum HOI/OI⁻ absorption, i.e. in the range 220–225 nm.

The measured absorption A_{obs}(λ) is the sum of the absorptions A_{HOI}(λ) and A_{OI⁻}(λ), which can be attributed to the two species HOI and OI⁻:

$$\begin{aligned} A_{\text{obs}}(\lambda) &= A_{\text{HOI}}(\lambda) + A_{\text{OI}^-}(\lambda) \\ &= \epsilon_{\text{HOI}}(\lambda)l[\text{HOI}] + \epsilon_{\text{OI}^-}(\lambda)l[\text{OI}^-] \end{aligned} \quad (7)$$

$$K_a = \frac{[\text{OI}^-][\text{H}^+]}{[\text{HOI}]} \quad (8)$$

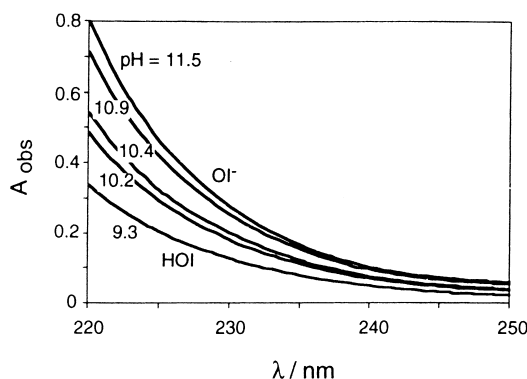


Fig. 1. UV absorbance spectra (200–250 nm) of 345 μM HOI/OI⁻ at varying pH values (9.3–11.5); pathlength 5 mm; I = 50 mM (phosphate buffer); T = 25°C.

Taking the acid-base equilibrium of HOI [equation (8)] into account, the following equation results:

$$\begin{aligned} \frac{A_{\text{obs}}(\lambda)}{l[\text{HOI}]_{\text{tot}}} &= \epsilon_{\text{HOI}}(\lambda) + K_a \frac{1}{[\text{H}^+]} \left(\epsilon_{\text{OI}^-}(\lambda) \right. \\ &\quad \left. - \frac{A_{\text{obs}}(\lambda)}{l[\text{HOI}]_{\text{tot}}} \right) \end{aligned} \quad (9)$$

Equation (9) describes the relation between the dissociation constant K_a, the observed absorbance A_{obs} (at a particular wavelength λ), the total iodine concentration [HOI]_{tot} = [HOI] + [OI⁻], the cell pathlength l, and the molar absorption coefficients of the pure species ε_{HOI} and ε_{OI⁻} (at a particular wavelength λ). If the term on the left hand side of equation (9) is plotted against the right hand side, a linear representation with K_a as slope results (see Fig. 2). According to Fig. 2 which shows the data measured at 220 nm, K_a can be calculated as 4.0 ± 0.7 × 10⁻¹¹ (pK_a = 10.4 ± 0.1). The intercept is the molar absorption coefficient of HOI at 220 nm, ε_{HOI}(λ = 220 nm). The ε_{HOI}(λ = 220 nm) determined by this procedure was 1650 M⁻¹ cm⁻¹. However, equation (9) has the restriction that the error increases with increasing pH when ε_{OI⁻}(λ) ≈ (A_{obs}(λ)/l[HOI]_{tot}). Therefore, this equation was only applied for the range of pH < 10.4. A slightly different equation which was also derived from equations (7) and (8) was used to interpret the data measured at pH > 10.4. For this pH range, ε_{OI⁻}-results as the intercept of the y-axis [ε_{OI⁻}(λ = 220 nm) = 5100 M⁻¹ cm⁻¹], while K_a⁻¹ is the slope (K_a = 4.2 ± 0.8 × 10⁻¹¹ calculated from A_{obs} at 220 nm).

K_a was calculated with both equations for A_{obs} at λ = 220 nm, λ = 222 nm, and λ = 225 nm and for [HOI]_{tot} = 23–460 μM. The pK_a was 10.4 ± 0.1 at 25°C with an ionic strength of 50 mM and did neither vary with the wavelength nor with [HOI]_{tot}. Within the errors given, both equations lead to the

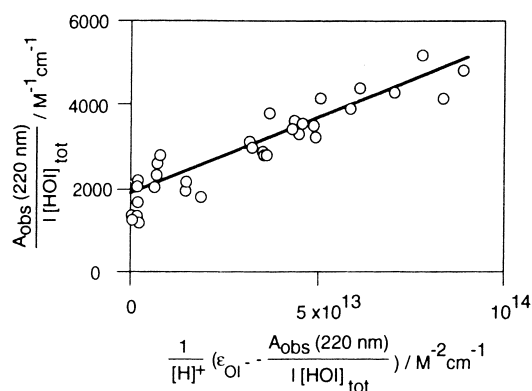


Fig. 2. Determination of the pK_a of HOI at 25°C and an ionic strength of 50 mM: Linearization of the absorbance data at 220 nm according to equation (9) (K_a = 4.0 ± 0.7 × 10⁻¹¹; r² = 0.868, n = 33).

same pK_a . The indicated error of pK_a represents the 95% confidence interval.

Previously, Chia calculated a value of 10.6 ± 0.8 with a combination of potentiometric and photometric methods (Chia, 1958). However, this value was based on indirect measurements, including the two equilibrium constants of equations (5) and (6) which are not very well known. In another study, a value of 10.0 ± 0.3 was estimated from a limited spectrophotometric data set at pH=4.0, 9.0, and 14.3 (Paquette and Ford, 1985). The pK_a determined in our study is within the range of the previous values. However, our direct measurements do not induce as many assumptions as the previous determinations.

Disproportionation kinetics of HOI/OI⁻

The decrease of HOI/OI⁻ (initial concentration 0.8–76 μM) in buffered solutions (pH=7.6–11.1) was measured spectrophotometrically (after reaction of HOI/OI⁻ to I₃⁻). Figure 3 shows the measured (symbols) and calculated (line) decrease of [HOI]_{tot}, together with the IO₃⁻ formation in a typical experiment (10 μM HOI, 25 mM borate at pH=8.0). IO₃⁻ which is formed according to equation (1) cannot exceed 1/3 of the initial [HOI]_{tot} (stoichiometric factor). The measured and calculated [IO₃⁻] [from HOI decrease according to equation (1)] are in almost perfect agreement (see Fig. 3). This is an independent confirmation of the assumed mechanism [equations (2–4)] in which the intermediate IO₂⁻ is rapidly oxidized to IO₃⁻.

The disproportionation of HOI/OI⁻ was always found to be second-order in [HOI]_{tot}. Hence, linear plots ($r^2 > 0.99$) could be observed if $1/[\text{HOI}]_{\text{tot}}$ was plotted against the reaction time t according to:

$$\frac{1}{[\text{HOI}]_{\text{tot}}} = \frac{1}{[\text{HOI}]_{\text{tot}}(t=0)} + k_{\text{obs}}t \quad (10)$$

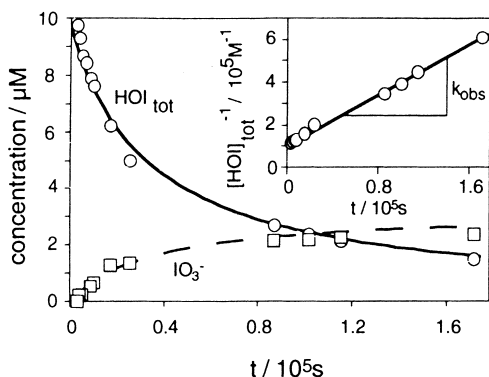


Fig. 3. Decrease of [HOI]_{tot} and formation of IO₃⁻ during the disproportionation of HOI/OI⁻. Inset: Linearization of the data according to equation (10) ($k_{\text{obs}}=2.95 \text{ M}^{-1} \text{ s}^{-1}$). Experimental conditions: [HOI]₀=10 μM ; pH=8.0, 25 mM borate; $T=25^\circ\text{C}$. Measured (symbols) and calculated (curves) data are shown.

The inset in Fig. 3 shows the linearization of the experimental data according to equation (10), with the observed rate constant k_{obs} as the slope.

HOI was usually produced by hydrolysis of I₂. However, when HOI was produced by oxidation of I⁻ by HOCl, this had no influence on k_{obs} .

k_{obs} was dependent on the pH and the buffer concentration. High pH and high buffer concentrations accelerated the disproportionation of HOI. To elucidate the importance of the buffer catalysis on the disproportionation, we performed experiments under varying buffer concentrations and at varying pH.

A buffer catalysis can occur via the acidic or the basic form of the buffer or through both species. In principle, several reactions can be catalyzed: HOI+HOI, HOI+OI⁻, and OI⁻+OI⁻. However, with the reaction OI⁻+OI⁻, we could not explain the pH-dependence of our experimental data. A reasonable fit of the data for borate and carbonate buffers was only achieved for two different mechanistic scenarios which cannot be distinguished from each other by our experiments. The first mechanism assumes that the basic form of the buffer is the active species and that two HOI molecules participate in the reaction. The second mechanism assumes that the protonated form of the buffer is the active species and that an HOI and an OI⁻ participate in the reaction. Chemical considerations led us to the assumption that the first mechanism is more likely than the second. We assume that the base interacts with the H-atom of HOI and thereby increases the nucleophile character of the I-atom. By this, the reactivity towards another HOI is enhanced.

As a result of this assumption, the following rate law for the base-catalyzed disproportionation can

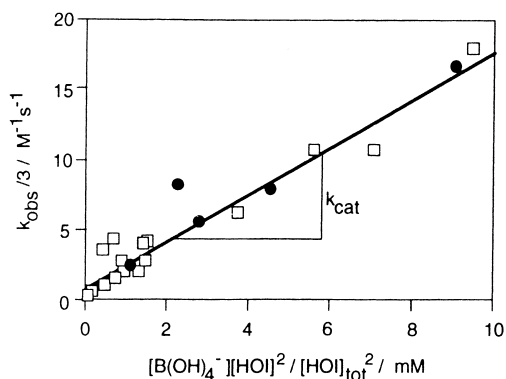


Fig. 4. Experimental data and linear least-squares fit for the disproportionation of HOI in the presence of borate according to equation (11). The linearity of the plot shows that the postulated equation (11) is in agreement with experimental findings. (□): data from this study; (●): data from Buxton and Sellers (Buxton and Sellers, 1985); $k_{\text{cat, borate}}=1700 \pm 600 \text{ M}^{-2} \text{ s}^{-1}$ with $r^2=0.992$ ($n=29$). Experimental conditions: pH=7.6–10.6; total borate concentration=2–25 mM; $T=25^\circ\text{C}$.

Table 1. Rate constants for the disproportionation of HOI/OI⁻ for varying reaction conditions at 25°C from this study

Equation number	Reaction	Rate constant (M ⁻¹ s ⁻¹)	[base]=5 mM (M ⁻¹ s ⁻¹)
(2)	HOI+HOI (<i>k</i> ₁)	0.3 ± 0.2	
(3)	HOI+OI ⁻ (<i>k</i> ₂)	15 ± 1	
(13)	HOI+HOI+HCO ₃ ⁻	50 ± 20 M ⁻² s ⁻¹	0.25 ± 0.1
(14)	HOI+HOI+CO ₃ ²⁻	5000 ± 500 M ⁻² s ⁻¹	25 ± 2.5
(15)	HOI+HOI+B(OH) ₄ ⁻	1700 ± 600 M ⁻² s ⁻¹	8.5 ± 3

be postulated:

$$\begin{aligned} -\frac{1}{3} \frac{d[\text{HOI}]_{\text{tot}}}{dt} &= \frac{1}{3} k_{\text{obs}} [\text{HOI}]_{\text{tot}}^2 \\ &= k_1 [\text{HOI}]^2 + k_2 [\text{HOI}][\text{OI}^-] + k_{\text{cat}} [\text{base}][\text{HOI}]^2 \end{aligned} \quad (11)$$

The factor of 1/3 corresponds to the stoichiometric factor of HOI in equation (1). Figure 4 shows a plot of $k_{\text{obs}}/3$ versus $[\text{base}][\text{HOI}]^2/[\text{HOI}]_{\text{tot}}^2$ for experiments with varying buffer concentrations (borate) and varying pH values (squares, for circles see below). The linearity of the plot shows that the postulated equation (11) is in agreement with experimental findings. The catalysis constant k_{cat} corresponds to the slope of the straight line. k_{cat} values for B(OH)₄⁻, HCO₃⁻, and CO₃²⁻ at 25°C are shown in Table 1. The k_{cat} values increase with increasing basicity of the buffer anions, $k_{\text{CO}_3^{2-}} > k_{\text{B(OH)}_4^-} > k_{\text{HCO}_3^-}$. An anion with a high basicity, such as CO₃²⁻, can interact more strongly with the H-atom of HOI than an anion with a lower basicity, such as HCO₃⁻. The interaction of the base with the proton in HOI leads to asymmetry (partial formation of OI⁻-like compound) which results in faster reaction.

Another compound which influenced the rate of the disproportionation was NH₄⁺/NH₃. However, in contrast to borate and carbonate, ammonia did not catalyze the reaction but an inhibition was observed. At pH=9.0, ammonia concentrations of 10–25 mM reduced k_{obs} by 50–80%. This effect could be related to the fact that NH₃ is a nitrogen base and not an oxygen base like the other bases which were investigated in this study. According to the HSAB-concept (Hard and Soft Acids and Bases), nitrogen bases are softer than oxygen bases (Pearson, 1969). HOI has a hard part (H-atom) and a soft part (I-atom). Nitrogen bases might therefore rather interact with the I-atom of HOI, whereas oxygen bases might rather interact with the H-atom. This difference could be a reason for the variation of the behavior with respect to the catalysis of the disproportionation.

The two rate constants for the uncatalyzed reactions HOI+HOI [equation (2)] and HOI+OI⁻ [equation (3)], k_1 and k_2 , were deduced from measurements at different pH-values and buffer concentrations by a regression analysis according to equation (12). Equation (12) was derived from

equations (8) and (11) under the restriction that $[\text{HOI}]_{\text{tot}} = [\text{HOI}] + [\text{OI}^-]$.

$$\frac{k_{\text{obs}}[\text{HOI}]_{\text{tot}}^2}{3[\text{HOI}]^2} - k_{\text{cat}}[\text{base}] = k_1 + k_2 \frac{K_a}{[\text{H}^+]} \quad (12)$$

Figure 5 shows a representation of equation (12). The slope of the straight line corresponds to k_2 , the y-axis intercept is k_1 . For the determination of k_1 , only the points at pH < 9 (low $K_a/[\text{H}^+]$) were used (see inset Fig. 5) since the reaction HOI+HOI only contributes significantly to the total reaction at pH < 9. The values of k_1 and k_2 are reported in Table 1. Because of the higher asymmetry between nucleophile and electrophile in the reaction HOI+OI⁻, k_2 is larger than k_1 . Therefore, a maximum rate for the uncatalyzed reaction can be expected at pH = pK_a = 10.4. A comparison of the rate constants for the catalyzed and the uncatalyzed reactions shows that at concentrations of 5 mM HCO₃⁻/CO₃²⁻ or 4 mM B(OH)₄⁻ at pH=8, the rate of the catalyzed and of the uncatalyzed reaction are in the same order of magnitude (Table 1).

Compared to literature values, our k_1 and k_2 values are quite small. This is due to the fact that in some previous calculations the catalytic effect of the basic form of the buffer was not taken into consideration (Thomas *et al.*, 1980; Truesdale *et al.*, 1994). This led to high k_1 and k_2 values because the

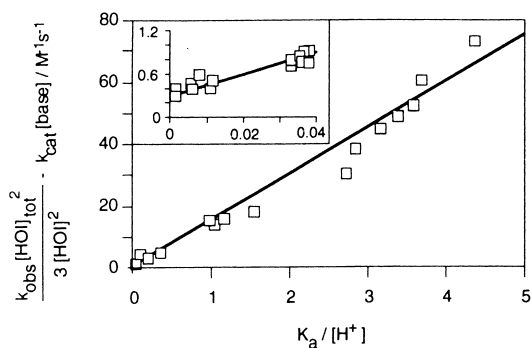


Fig. 5. Determination of the rate constants k_1 and k_2 for the uncatalyzed reactions HOI+HOI and HOI+OI⁻ according to equation (12). k_2 is the slope of the main linear curve ($r^2=0.977$, $n=15$). The inset shows the points which were used for the determination of k_1 (y-axis intercept), $r^2=0.911$ ($n=14$). Experimental conditions: pH=7.6–11.1; $[\text{HOI}]_{\text{tot}}=0.8\text{--}76\ \mu\text{M}$; carbonate and borate buffers (2–30 mM); $T=25^\circ\text{C}$.

total disproportionation of both catalyzed and uncatalyzed reactions was attributed to k_1 and k_2 . Buxton and Sellers (1985), however, allowed for the catalytic effect of borate. Their raw data (pH = 9.1–9.7, 2–50 mM total borate) fit very well in our data set, as is shown in Fig. 4 by the circles. We have evaluated their raw data according to equation (11) and have found a k_{cat} value of $1400 \pm 300 \text{ M}^{-2} \text{ s}^{-1}$ ($r^2 = 0.927$). This value is in agreement with our result [Table 1, equation (15)].

Implications for drinking water treatment

In oxidative drinking water treatment, HOI formed from the oxidation of I^- can have various fates which are kinetically determined. One possibility is the formation of undesired iodoorganic compounds such as CHI_3 , which leads to a bad taste and odor of the drinking water. Our results allow us to estimate the life-time of HOI/OI^- if disproportionation is the main reaction pathway.

The initial half-life of HOI has been calculated for different conditions (Table 2). Because the disproportionation is second-order in HOI/OI^- , the half-life of HOI depends strongly on its initial concentration. A ten-fold increase of $[\text{HOI}]$ ($t = 0$) results in a ten-fold decrease of the half-life. An increase in the pH from 6 to 9 leads to an increase in the reaction rate because the speciation is shifted towards OI^- which reacts faster than HOI. In the presence of carbonate, the reaction rate is further increased because of the catalysis of HCO_3^- and CO_3^{2-} . According to Table 2, the initial half-life of HOI under drinking water relevant conditions (1–10 $\mu\text{g l}^{-1}$ HOI, pH = 6–8, 0–5 mM carbonate) is in the order of 50–1300 days. The time for a 90% removal of HOI is nine times higher. Even under extreme conditions (100 $\mu\text{g l}^{-1}$ HOI, pH = 9, 5 mM carbonate), the initial half-life is never lower than approximately two days. We can therefore conclude that the disproportionation of HOI/OI^- is too slow under drinking water conditions to be of importance for the fate of HOI. The fate of HOI during drinking water treatment and distribution will therefore be determined by its reaction with NOM and its further oxidation to IO_3^- .

Table 2. Initial half-life in days of HOI at varying HOI concentrations, pH, and carbonate concentrations

[HOI]/ $\mu\text{g l}^{-1}$	[carbonate]/mM	$t_{1/2}/\text{d}$			
		pH = 6	pH = 7	pH = 8	pH = 9
1	0	1300	1300	1100	500
10	0	130	130	110	50
100	0	13	13	11	5.0
1	5	700	680	540	190
10	5	70	68	54	19
100	5	7.0	6.8	5.4	1.9

CONCLUSIONS

- The pK_a of HOI was determined to be 10.4 ± 0.1 . Therefore, under typical drinking water conditions, HOI is the major species, whereas OI^- is only a minor species.
- The uncatalyzed disproportionation of HOI occurs through the reactions $\text{HOI} + \text{HOI}$ and $\text{HOI} + \text{OI}^-$ at pH = 7.6–11.1. Bicarbonate, carbonate, and borate catalyze the disproportionation. We postulate that the catalysis is particularly important for the reaction $\text{HOI} + \text{HOI}$.
- Although catalyzed by carbonate, the disproportionation of HOI is slow under typical drinking water treatment conditions (pH = 6–8). The initial half-life of HOI lies in the order of a few days to years. Therefore, the life-time of HOI is not controlled by this reaction. During oxidative drinking water treatment, the fate of HOI is determined either by its further oxidation by an oxidant or by the reaction with NOM. The competition of these two reaction pathways determines the importance of the two final products which are IO_3^- or iodoorganic compounds.

Acknowledgements—Financial support from Suez Lyonnaise des Eaux for YB is acknowledged. The authors thank J. Hoigné for discussions and the thorough review of the manuscript. We are grateful to E. Salhi and Y. Oliveras for their technical support.

REFERENCES

- Awtrey A. D. and Connick R. E. (1951) The absorption spectra of I_2 , I_3^- , I^- , IO_3^- , $\text{S}_4\text{O}_6^{2-}$, and $\text{S}_2\text{O}_3^{2-}$. Heat of the reaction $\text{I}_3^- = \text{I}_2 + \text{I}^-$. *J. Am. Chem. Soc.* **73**, 1842–1843.
- Bichsel Y. and von Gunten U. (1999a) Oxidation of iodide and hypiodous acid in the disinfection of natural waters. *Environ. Sci. Technol.* **33**, 4040–4045.
- Bichsel Y. and von Gunten U. (1999b) Determination of iodide and iodate by ion chromatography with postcolumn reaction and UV/Visible detection. *Anal. Chem.* **71**(1), 34–38.
- Bruchet A., N'Guyen K., Mallevalle J. and Anselme C. (1989) Identification and behaviour of iodinated haloform medicinal odor. In *Proceedings of AWWA Seminar on Identification and Treatment of Taste and Odor Compounds*, Los Angeles, CA, pp. 125–141.
- Burger J. D. and Liebafsky H. A. (1973) Thermodynamic data for aqueous iodine solutions at various temperatures. *Anal. Chem.* **45**(3), 600–602.
- Buxton G. V. and Sellers R. M. (1985) Radiation-induced redox reactions of iodine species in aqueous solution. *J. Chem. Soc., Faraday Trans.* **81**, 449–471.
- Chia Y. (1958) Chemistry of +I iodine in alkaline solution. Thesis University of California, Berkeley.
- Fabian I. and Gordon G. (1997) The kinetics and mechanism of the chlorine dioxide–iodide ion reaction. *Inorg. Chem.* **36**, 2494–2497.
- Fuge R. and Johnson C. C. (1986) The geochemistry of iodine—a review. *Environ. Geochem. Health* **8**(2), 31–54.
- Garland J. A., Elzerman A. W. and Penkett S. A. (1980)

- The mechanism for dry deposition of ozone to seawater surfaces. *J. Geophys. Res.* **85**(C12), 7488–7492.
- Hansson R. C., Henderson M. J., Jack P. and Taylor R. D. (1987) Iodoform taste complaints in chloramination. *Water Res.* **21**(10), 1265–1271.
- Kumar K., Day R. A. and Margerum D. W. (1986) Atom-transfer redox kinetics: general-acid-assisted oxidation of iodide by chloramines and hypochlorite. *Inorg. Chem.* **25**(24), 4344–4350.
- Myers O. E. and Kennedy J. W. (1950) The kinetics of iodine-iodate isotopic exchange reaction. *J. Am. Chem. Soc.* **72**, 897–906.
- Nagy J. C., Kumar K. and Margerum D. W. (1988) Non-metal redox kinetics: oxidation of iodide by hypochlorous acid and by nitrogen trichloride measured by the pulsed-accelerated-flow method. *Inorg. Chem.* **27**(16), 2773–2780.
- Paquette J. and Ford B. L. (1985) Iodine chemistry in the +1 oxidation state. I. The electronic spectra of OI⁻, HOI, and H₂OI⁺. *Can. J. Chem.* **63**, 2444–2448.
- Pearson R. G. (1969) Hard and soft acids and bases. *Survey of Progress in Chemistry* **5**, 1–52.
- Soulard M., Bloc F. and Hatterer A. (1981) Diagrams of existence of chloramines and bromamines in aqueous solution. *J. Chem. Sol., Dalton Trans.* **12**, 2300–2310.
- Suez Lyonnaise des Eaux (1993) Conditions de formation et destruction des trihalométhanes iodés responsables des goûts et odeurs pharmaceutiques. Lyonnaise des Eaux, Internal Report.
- Thomas T. R., Pence D. T. and Hasty R. A. (1980) The disproportionation of hypoiodous acid. *J. Inorg. Nucl. Chem.* **42**, 183–186.
- Truesdale V. W., Canosa-Mas C. and Luther III G. W. (1994) Kinetics of disproportionation of hypoiodous acid. *J. Chem. Soc., Faraday Trans.* **90**(24), 3639–3643.
- Truesdale V. W. and Canosa-Mas C. (1995) Kinetics of disproportionation of hypoiodous acid in phosphate and borate buffer at pH < 8.5 modelled using iodide feedback. *J. Chem. Soc., Faraday Trans.* **91**(15), 2269–2273.
- Truesdale V. W. (1997) Kinetics of disproportionation of hypoiodous acid at high pH, with an extrapolation to rainwater. *J. Chem. Soc., Faraday Trans.* **93**(10), 1909–1914.
- Urbansky E. T., Cooper B. T. and Margerum D. W. (1997) Disproportionation kinetics of hypoiodous acid as catalyzed and suppressed by acetic acid-acetate buffer. *Inorg. Chem.* **36**, 1338–1344.
- Wren J. C., Paquette J., Sunder S. and Ford B. L. (1986) Iodine chemistry in the +1 oxidation state. II. A Raman and UV-Visible spectroscopic study of the disproportionation of hypoiodite in basic solutions. *Can. J. Chem.* **64**(12), 2284–2296.